



Airborne Geophysical Data Analysis of Serpentinites Occurrences in Morro Feio Ultramafic Complex, Tocantins Province, Goiás, Brazil

Adolfo Barbosa da Silva, Tiago Rocha F. Duque and Felipe da Mota Alves, Brazilian Geological Survey (SGB/ CPRM)

Copyright 2017, SBGf - Sociedade Brasileira de Geofísica.

This paper was prepared for presentation during the 15th International Congress of the Brazilian Geophysical Society held in Rio de Janeiro, Brazil, 31 July to 3 August, 2017. Contents of this paper were reviewed by the Technical Committee of the 15th International Congress of the Brazilian Geophysical Society and do not necessarily represent any position of the SBGf, its officers or members. Electronic reproduction or storage of any part of this paper for commercial purposes without the written consent of the Brazilian Geophysical Society is prohibited.

Abstract

Using airborne geophysical data combined with geological information was possible to locate areas with potential for serpentinite occurrences in the Morro Feio Ultramafic Complex, Goiás States. The potential areas mapped in this study were characterized as $eU / eTh \geq 1$, magnetometric anomalies with SI between 1.00 - 2.63, depths between 130 -550 m and occurring at ned topography sites. If such serpentinite occurrences are proven in later studies, the areas mapped in the present work may be a target for mineral prospecting in the studied region, since the serpentinites is the primary source of surface chromite and garnierite occurrences known in the region.

Introduction

Ultramafic complexes are composed of varying proportions of harzburgite, lherzolite and dunite, usually with metamorphic textures (more or less serpentinitized) and may contain important sources of Zn, Cu, Co, Ni, Cr, Au, and PGE's (Coleman, 1977; Castroviejo et al., 2004 apud Queiroga et al., 2012). In Brazil, a considerable portion of the ultramafic complexes occurs mainly in the Tocantins Province, and about 180 ultramafic massifs have been known in the Goiás State since the 1970s. Some of these massifs were classified by Berbert (1977) as serpentinitized dunites / peridotites of the Morro Feio alpine type.

The Morro Feio is located at northerly of the Hidrolândia city (30 km south of the Goiás Capital), near the highway BR - 153 that connects Goiânia to São Paulo. It is an elevation with about 940 m of altitude, 4 km of length in northward, 2 - 2.5 km wide, (Berbert and Mello, 1969). Previous work has identified important mineral occurrences (mainly of chromite and garnierite) associated to surface deposits generated from the laterization process and concretion of serpentinites (Berbert and Mello, 1969; Milliotti, 1978). However, due to the irregular character of these occurrences and the ease of exploration, the plots, mainly of chromite, are in the process of exhaustion (Valente, 1986). Therefore, it is necessary to use new techniques that may indicate new targets for mineral prospecting, especially with regard to serpentinite mapping, as these may constitute a primary source for Cr and Ni mineralization. In this context, it is worth highlighting

the contributions airborne geophysical data can provide in this stage of knowledge.

The objective of the present study is to present the the processing results, interpretation and integration of airborne geophysical data with the existing geological data in order to propose the location of possible serpentinite bodies that may be related to the mineral occurrences at Morro Feio Ultramafic Complex (MFUC).

Geological Context

The studied area (Figure 1) is located in the south - center portion of the Tocantins Province. This province is a Neoproterozoic geotectonic entity developed as a result of the convergence and collision between the Amazonian, São Francisco-Congo Cratons (Dardenne, 2000; Lacerda Filho et al., 2003) and a third crustal block known as Paranapanema (Mantovani & Brito Neves, 2009). Among the several tectonic units that compose the Tocantins Province, it is of interest the tectonic unit known as Brasília Belt. This unit is fold-and-thrust belt characterized by associations of supracrustal deformed rocks along the western flank of the San Francisco Craton. In the internal portion of the Brasília Belt (Lacerda Filho et al., 2003), or meridional (Dardenne, 2000), the Araxá Group metasedimentary rocks occur. In the study area, the Araxá Group metasediments are basically formed by garnet - mica schists, quartz - mica schists and micaceous quartzite. Hosted in these units is the MFUC.

Milliotti (1978) divided MFUC described by Berbert and Mello (1967) into five units: A1 - Serpentinites, formed by antigorite, chrysotile and xenomorphic magnetite and leucoxene. The presence of olivine grain is doubtful; A2 - Corresponds to unit A1 silicified; B1 - formed by antigorite, talc and magnetite; B2 - formed by talc, magnetite in euhedral porphyroblasts, antigorite, chlorite and actinolite in centimetric crystals, fibroradiated, and magnesite in porphyries; C - formed by chlorite, magnetite in euhedral porphyroblasts of up to 2 cm, epidote, talc, tremolite, in fibroradiated porphyroblasts, and black tourmaline in fibroradiated porphyroblasts and euhedral. Berbert and Mello (1969) also identified a dike with direction of N30W, 3km long and 100m wide cutting the Araxá Group rocks. The dike is composed of calcium plagioclase, pyroxenes and magnetite and ilmenite as accessory minerals. Finally, we have the surface deposits that correspond to the alluvium and eluvium already mentioned above. These surface deposits are important from the economic point of view because they contain significant amounts of chromite (Milliotti, 1978).

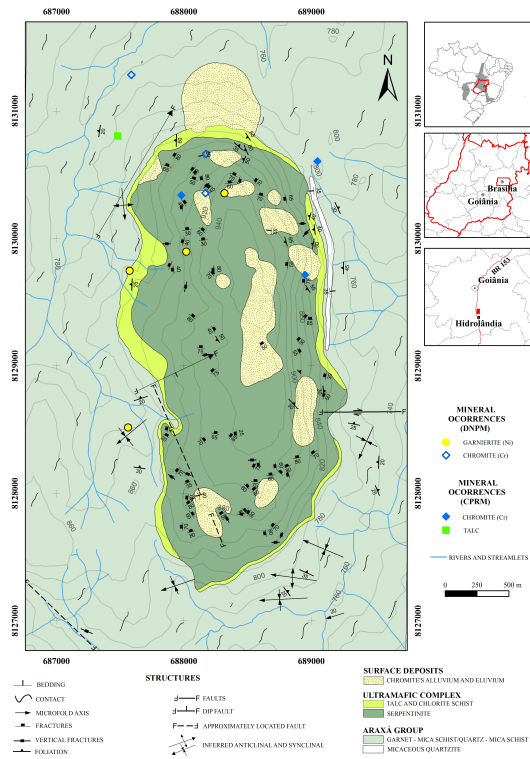


Figure 1: Geological map of the surroundings of the MFUC presenting the mineral occurrences cataloged by DNPM (Berbert & Mello, 1967) and CPRM (Lacerda Filho et al., 2000). Modified by Berbert & Mello (1967).

Methodology

The aerogeophysical data used are part of the Brasília South Aerogeophysics Project, acquired in 2005 by the Prospecting & Engineering Lasa company and are in the domain of CPRM. The flight and ties lines spacings were 500 m in the N - S direction and 10 km in the E - W direction, respectively. The nominal flight height was 100 m. Geosoft® Oasis Montaj™ 9.0.2 software was used in the processing stage. In this step, the aerogeophysical data were projected for the UTM Zone 22S coordinate system and SIRGAS 2000 datum, and then the magnetometric data were interpolated by the bi-directional method with 100 m cell size (Billing & Richards, 2001) and it was obtained the Total Magnetic Intensity (TMI). The analytical signal amplitude (ASA) (Nabighian, 1972; Roest et al., 1992) was applied to TMI to centralize magnetic anomalies (McLoad et al., 1993). In order to reduce the possible effects of high frequency noise, an upward continuation of 100m was calculated from the ASA and then were produced the first and second order vertical derivatives (FVDR and SVDR), Total Horizontal Derivative (THDR) (Cordell & Gauch, 1985), Tilt angle (TDR) (Miller & Singh, 1994) and Total Horizontal Derivative of the Tilt angle (THDR - TDR) (Verduzco et al., 2004) maps.

A statistical analysis have performed on gamma ray spectrometry data and was identified negative values corresponding about 3% of the total counts and 5.6%, 5.0% and 24.4% of the potassium (K), thorium equivalent (eTh) and uranium equivalent (eU) concentrations. It following Grant's (1998) suggestion, the negative data

were kept in the database and was added a constant of 2.5 in the channels mentioned. This procedure was intended to make that all values were positives so that qualitative analysis based on the ratios between the radioelements were possible. The addition of a constant in the mentioned channels did not affect the shape of the profiles (figure 2). Then gamma ray spectrometry data were interpolated using the minimum curvature method, with cell size of 100 m (Billing & Richards, 2001) and were obtained the K, Th and eU concentrations maps and the eU/eTh, eU/K, K/eTh ratios maps. Finally, a 90 m resolution digital elevation model (DEM) acquired by Shuttle Radar Topography Mission (SRTM) was used to support subsequent interpretations.

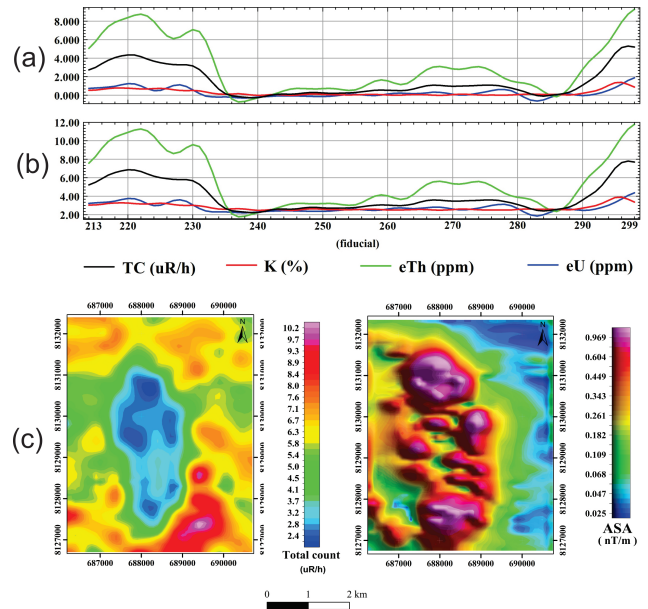


Figure 2: Profiles of the radioelements concentration before (a) and after (b) the addition of a constant. c) Total count and ASA map.

Results

Generally, the thematic maps produced have a low radiometric count and high magnetic signal (Figure 2b and 2c). However, when we observed radiometric ratios maps and SVDR, TDR and THDR - TDR maps, it was possible to identify some areas whose gamma - ray spectrometric and magnetometric showed peculiars responses. In order to investigate these areas in more detail, six profiles were analyzed along the flight lines (L1 - L6) and a profile along the ties line (L7) (Figure 3).

A total of eight "anomalous" areas (G1 - G8) were quantified using the profiles presented in figure 3, where the eU concentration was relatively higher than that of eTh and 17 areas (M1 - M17) classified as magnetometric anomalies, where one positive peak in the value of TDR and SVDR is observed in agreement with a local minimum value of the THDR - TDR and this set being limited at both ends by approximately two positive peaks in the value of the THDR - TDR (Verduzco et al, 2004; Ferreira et al., 2010).

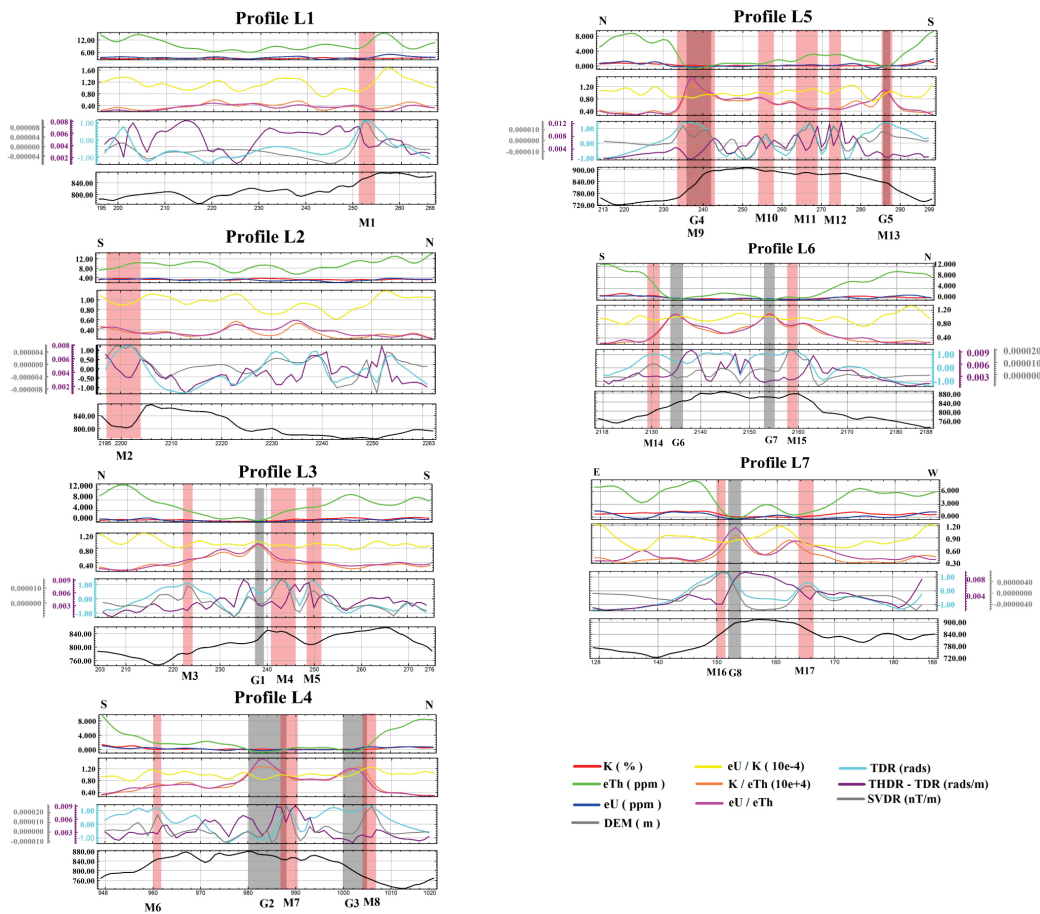


Figure 3: Flight (L1 - L6) and ties lines (L7) profile. Horizontal axis = fiducial.

Some estimates of depth values and structural indices (SI) for magnetometric anomalies were also made and are presented in table 1. These estimates were obtained through the methodology of Salem & Ravat (2003) that use the ASA combination with the Euler deconvolution. This table also shows possible associations between magnetometric anomalies and gamma ray spectrometry "anomalies".

Table 1: Depth and SI values calculated for magnetometric anomalies. Error estimated in the depth value: 10%.

Magnetometrics anomalies	Gamaespectrometrics anomalies	Depth (m)	Structural Index (SI)
M1	-	189±19	1.45
M2	-	-	-
M3	-	52±5	0.05
M4	G1	190±19	1.00
M5	-	252±25	1.17
M6	-	78±8	0.35
M7	G2	172±17	1.90
M8	G3	107±11	0.47
M9	G4	537±54	2.63
M10	-	-	-
M11	-	197±20	2.29
M12	-	122±12	1.34
M13	G5	212±21	0.82
M14	G6	135±14	0.88
M15	G7	262±26	1.97
M16	G8	140±14	0.69
M17	-	-	-

Table 2: Grouping of solutions from table 1.

Group	Magnetometrics anomalies	SI	Depth (m)
1	M3 and M6	< 0.50	<100
2	M1, M5, M11 and M12	1.00 – 2.50	100 – 200
3	M4, M7, M8, M9, M13, M14, M15 and M16	0.50 – 2.75	100 - 550

Analyzing table 1, the solutions are grouped into three large groups (table 2). All anomalies can be considered with shallow depths, with values of depths less than 550 m. Only in group 3 all magnetometric anomalies are associated with gamma ray spectrometry "anomalies". The M9 magnetometric anomaly is noteworthy, since it has the highest SI and depth calculated and is associated with one of the most extensive gamma ray spectrometry "anomalies" (see profile L5). Near the M9 anomaly there are two chromite occurrences and one garnierite occurrence (Et. al, 1969; Milliotti, 1978). There are also garnierite occurrences near the M7 and M4 anomalies and there are chromite occurrences near the M8 and M15 anomalies (Figure 4).

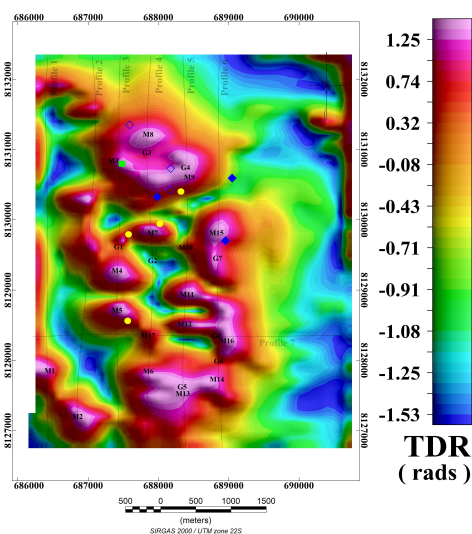


Figure 4: Map showing the locations of the gamma ray spectrometry “anomalies” and magnetometric anomalies and mineral occurrences. The symbols of the mineral occurrences are the same as in figure 1.

These characteristic make group 3 anomalies a target for research. In the other groups, the proximity between magnetometric anomalies and mineral occurrences showed a little correlation, with the exception of the M3 anomaly group 1) that practically coincides with an talc occurrence and the M5 anomaly (group 2) that is close to one garnierite occurrences (Berbert and Mello, 1969; Milliotti, 1978) (Figure 4).

Discussions and Conclusions

Based on the work done by Strieder & Nilson (1992) and Strieder & Nilson (1992b), in which these authors identified a set of serpentinitized mafic and ultramafic rocks housed in the metasediments Araxá Group near Abadiânia City, about 90 km NE of the MFUC, it can be concluded that:

- The process of serpentinitization and metasomatism occurred simultaneously during the main deformation phase.
- Through intergranular diffusion, Si^{+4} , Al^{+3} and LREE were transferred to the serpentinite, while Mg^{+2} was transferred to the garnet-mica schist. The Ni^{+2} , Cr^{+3} , Co^{+3} , Ti^{+4} species remained immobile during metasomatism.
- The serpentinite protolith has a harzburgitic composition.
- The mafic-ultramafic-metasediments set rocks in Abadiânia could possibly be part of an ophiolitic mélange unit and its area of occurrence expands beyond for that city. In this context, the MFUC is an exotic block isolated in the garnet - mica schist of the Araxá Group.

Another important study was done by Deschamps et al. (2013). These authors analyzed the geochemical signature

of ~900 serpentinite samples and concluded that:

- The major elements are preserved during the hydration process, but the talc can modify the composition of these elements, notably by Si enrichment.
- Serpentinites derived from harzburgite or lherzolite commonly have $MgO / SiO_2 < 1.1$ ratio.
- Serpentinites related to subduction, with antigorite, have an $Al_2O_3 / SiO_2 > 0.03$ ratio and are more enriched in trace elements (LREE) than the abyssal and mantle wedge serpentinites. Such enrichments may indicate that the protoliths of the subduction-related serpentinites were enriched in a supra-subduction environment by fluids during hydration.
- The serpentinite total rock geochemistry is characterized by an enrichment of U without significant enrichment in Th.

From these considerations, the results of the chemical analysis of the total rock of the serpentinites and associated lithologies by Milliotti (1978) (Table 3) were used.

In Table 3, Milliotti (1978) had already observed that the samples of serpentinites (A1 and B1 units) had certain chemical similarities, mainly in relation to Si that ranges from 39.2% to 42.0% in these rocks, except for the MFCA-23, which corresponds to the portion of the silicified serpentinite. Such silicification could reflect the Si transfer mechanism, as pointed out by Strieder & Nilson (1992b) and Deschamps et. al (2013).

We can also observe in Table 3 that the mean MgO / SiO_2 ratio of the serpentinites is 0.90. This value, according to the conclusion of Deschamps et. al (2013) could indicate a harzburgitic protolith for the MFUC's serpentinites. This hypothesis would be in agreement with the results obtained by Strieder & Nilson (1992a).

In addition, the Al_2O_3 / SiO_2 ratios of these units, around 0.04, suggest that MFUC's serpentinites could be classified as serpentinites related to subduction. If this hypothesis is valid, the LREE enrichment mentioned by Deschamps et al. (2013) could be explained by the intergranular diffusion mechanism suggested by Strider & Nilson (1992b) who also verified LREE enrichment in the Abadiânia serpentinites.

Considering the above correlations we can postulate that the MFUC's serpentinites could also be characterized by U enrichment without a pronounced Th enrichment. By observing the gamma ray spectrometry “anomalies” in the profile, it's are found to be more characterized by a drop in eTh concentration than an increase in eU concentration, arriving being lesser than it. It is noteworthy that this fall in eTh concentration occurs in terrain with accentuated inclined topography, that is, where the erosion process is predominant. In this scenario, the gamma ray spectrometry response would be reflecting the lower layers possibly associated with the bedrock (Wildfort et al., 1997).

Table 3: Total rock chemical analyze at MFUC's serpentinites and associated lithologies. Methodology used: optical spectroscopy and atomic absorption. Accuracy of 0.02%. Modified by Milliotti (1978).

Samples	Oxides (%wt)														Elements (ppm)				
	SiO ₂	Al ₂ O ₃	Fe ₂ O ₃	FeO	MgO	MnO	CaO	Na ₂ O	K ₂ O	TiO ₂	P ₂ O ₅	CO ²⁺	H ₂ O	S	Total	Cl	F	Cr	Ni
MFCA - CR - 1 - A	39.9	2.9	7.3	1.48	35.9	0.15	0.03	<0.01	0.04	0.06	<0.03	<0.05	11.08	<0.01	98.93	30	30	3350	2170
MFCA - 30 - A	40.5	1.7	7.4	2.75	37.0	0.17	0.03	<0.01	0.06	0.05	<0.03	0.05	10.35	<0.01	100.11	30	67	2760	1800
MFCA - 23	68.9	1.5	8.2	2.82	13.8	0.41	0.03	<0.01	0.04	0.06	0.03	0.38	3.70	<0.01	99.55	30	40	670	1420
MFCA - 13	41.6	2.1	6.7	1.56	35.6	0.11	0.06	< 0.01	0.07	0.05	< 0.03	0.05	0.05	< 0.01	99.16	30	68	2100	1040
MFCA - 14	39.2	1.8	8.6	2.45	36.2	0.11	0.04	<0.01	0.07	<0.05	<0.03	<0.05	10.56	<0.01	99.18	30	30	3600	1600
MFCA - 15 - A	40.2	1.6	6.8	2.30	37.1	0.11	0.05	<0.01	0.09	0.06	<0.03	<0.05	10.53	<0.01	98.94	30	30	3000	1740
MFCA - 17	40.3	1.6	4.2	2.23	38.0	0.11	0.04	<0.01	0.06	0.06	<0.03	0.16	12.25	<0.01	99.06	30	30	2600	2600
MFCA - 40	41.5	1.6	4.3	4.16	36.3	0.11	0.03	<0.01	0.04	0.06	<0.03	0.05	10.82	<0.01	100.11	30	67	2760	1800
MFCA - 44 - A	39.9	1.5	6.2	2.6	37.9	0.16	0.04	<0.01	0.04	0.06	<0.03	<0.05	10.82	<0.01	99.46	30	53	2600	2600
MFCA - 56	40.3	1.4	7.1	1.49	36.8	0.08	0.06	<0.01	0.06	0.08	<0.03	<0.05	11.43	<0.01	98.90	30	125	2900	1320
MFCA - 44 - C	42.0	1.7	8.9	1.93	34.1	0.19	0.04	<0.01	0.04	0.06	<0.03	<0.05	10.46	<0.01	99.52	30	133	2500	2400
MFCA - 39 - B	26.2	21.6	3.5	12.61	22.9	0.25	0.03	<0.01	0.01	1.9	<0.03	<0.05	10.57	<0.01	99.67	30	30	400	370
MFCA - 39 - C	51.8	2.3	11.8	1.48	25.0	0.16	0.04	<0.01	0.04	0.16	0.03	0.05	5.55	<0.01	98.43	30	155	4500	2850

 A1 Unit – Serpentinite

 A2 Unit – Silicified serpentinite

 B1 Unit – Talc – bearing serpentinite

 B2 Unit – Talc schist with magnetite

 C Unit – Chlorite schist

 fractures filled with serpentinitic material in the B unit

These observations suggest that the location where the eU concentration is relatively larger than that of eTh is reflecting a lithology, in this case the serpentinite, rather than a process of alteration. Magnetometric anomalies may be associated with serpentinites and talc schist and/or chlorite schist. In the first case, magnetometric anomalies would be associated with gamma ray spectrometry “anomalies” (group 3). The group 3 anomalies have SI near or greater than 1.00, suggesting geometry of a vertical dike, or an irregular sill, for the magnetic source (Barbosa & Silva, 2005) and depths greater than 130 m. The exceptions are the M8 and M16 anomalies, which have an SI compatible with a contact zone and, therefore, may be related the serpentinite contact zones. The second case may be represented by the magnetometric group 1 anomalies. Evidence for this hypothesis is the occurrence of talc near the M3 anomaly.

Finally, the group 2 anomalies, M1, and possibly M2, appear to be associated with the dike mapped by Berbert and Mello (1969). This dike corresponds to a small linear segment of the mafic bodies that form the Azimuth 125 ° lineament. The calculated SI values are consistent with the SI values used by Moraes Rocha et al. (2014). Finally, the other group 2 anomalies and, possibly, the anomalies M10 and M17, may be related to the serpentinites. The absence of a gamma ray spectrometry response in these areas may be due to the fact that the M5, M10, M11 and M12 anomalies occur at relatively smooth slope topography sites, that is, where weathering is dominant. At these sites, serpentinites gamma ray spectrometry response may have been obliterated and reflecting the regolith rather than the serpentinite itself (Wildfort et al., 1997). In addition, these anomalies have SI and depths values very similar to those of group 3.

It was observed that Cr and Ni concentrations in Table 3 show that, as Milliotti (1978) concluded, the serpentinites are the units with the highest concentrations of these elements. The results described point to the location of potential areas for the serpentinites occurrence. It is suggested a study that takes into account the field data that can confirm the occurrence of such rocks in the areas in question, because, as these occur close to the sites where there has been mining of chromite from surface deposits, they may constitute a primary source of chromite and garnierite mineralization and could constitute important areas from the point of view of mineral exploration.

Through the processing and interpretation of airborne geophysical data and integration with existing geological data, as well as the use of studies, we conclude that the identified airborne geophysical responses possibly indicate potential areas for serpentinite bodies occurrence, which may contain Cr and Ni mineralization.

Acknowledgement

The authors are grateful to the Remote Sensing and Geophysics Division of the Mineral Resource Research Company / Geological Survey of Brazil for providing the aerogeophysical data that were used in the present work.

References

Berbet, C. O., Mello, J. C. R., 1969, investigação geológica - econômica da área de Morro Feio - Hidrolândia, Goiás, DNPM/DFPM, Bol. N° 132, 81p.

Berbert, C. O., 1977, Complexos máfico/ultramáficos no Brasil, In: I Simpósio de Geologia Regional, Atas...São Paulo (SP): SBG, p. 004 - 028.

- Billings, S. D., Richards, D.**, 2001, Quality control of gridded aeromagnetic data: *Exploration Geophysics*, v. 31, p.611-616.
- Barbosa, V. C. F., Silva, J. B.C.**, 2005, Deconvolução de Euler: passado, presente e futuro - um tutorial, *Revista Brasileira de Geofísica*, 23(3), p.243 - 250.
- Catroviejo, R.**, 2004, El oro en ofiolitas. In: Pereira, E., Castroviejo, R., Ortiz.,(eds). *Complejos Ofiolíticos em Iberoamérica: guías de prospección para metales preciosos*. Madrid: Rede CYTED., 379 p. cap., 2 p. 25 - 69.
- Coleman, R. G.**,1977, Ophiolites: Ancient Oceanic Lithosphere? *Mineral and Rocks* vol. 12, Springer - Verlag, p. 229.
- Dardenne, M. A.**, 2000. The Brasília Fold Belt. In: Cordani, U.G., Milani, E.J., Thomaz Filho, A., Campos Neto, D. A. (eds.). *Tectonic Evolution of South America*, Rio de Janeiro: 31st. IGC, 231-263.
- Deschamps, F., Godard, M., Guillot, S., Hattori, K.**, 2013, Geochemistry of subduction zone serpentinite, *Lithos*, Vol. 178, 96 - 127 p.
- Ferreira, F. J., Souza, J., Bongiolo, A. B. S., Castro, L. G., Romeiro, M. A. T.**, 2010, Realce do gradiente horizontal total de anomalia magnéticas usando a inclinação do sinal analítico. Parte I - Aplicação a dados sintéticos, IV Simpósio Brasileiro de Geofísica, Brasília - DF.
- Grant, J. A.**, 1998, Tem things the textbooks don't tell you about processing and archiving airborne gamma-ray spectrometrics data, *Geological Survey of Canada*, 83 - 87p.
- Lacerda Filho, J. V., Rezende, A., Silva, A.**, 2000. *Geologia e Recursos Minerais do Estado de Goiás e Distrito Federal*. Escala 1:500.000. Programa de Levantamentos Geológicos Básicos do Brasil - PLGB.Goiânia, CPRM/METAGO-SA/UnB, 176 p
- Lacerda Filho, J. V et al.**, 2003, Provincia Tocantins, Cap. V, In: Bizzi, L. A., Schobbenhaus, C., Vidotti, R. M., Golçalves, J.H (org.), *Geologia, Tectônica e Recursos Minerais do Brasil: Textos, Mapas & SIG*, Comp. De Pesq. Rec. Minerais/Serviço Geológico do Brasil.
- MacLoad, I. N., Jones, K., Dai, T. F.**, 1993, 3 - D Analytical signal in the interpretation of total magnetic fields data at low magnetic latitudes, *Exploration Geophysics*, 24, 679 - 688.
- Mantovani, M. S. M., Brito Neves, B. B.**, 2009. The Paranapanema lithospheric block: its nature and role in the accretion of Gondwana. In: Gaucher,C., Sial, A.N., Halverson, G.P., Frimmel, H.E.(Eds): *Neoproterozoic Cambrian Tectonics, Global Change and Evolution: a focus on southwestern Gondwana*. *Developments in Precambrian Geology*, 16, Elsevier, pp. 257-272.
- Miller, H. G., Singh,.,** 1994, Potential field tilt - A new concept for location of potential field sources: *Journal of Applied Geophysics*, 32, no. 2-3, 213-217.
- Milliotti, C. A.**, 1978, Distribuição e controles da mineralização de platina no Morro Feio - GO, Tese de Mestrado, Universidade de Brasília, 149 p.
- Moraes Rocha, L.G., Pires, A. C. B., Carmelo, A. C., Araujo Filho, J. O.**, 2014, Geophysical characterization of the Azimuth 125° lineament with aeromagnetic data: Contribution to the geology of central Brazil, *Precambrian Research*, 249, 273 ? 287p.
- Nabighian, M. N.**, 1972, The analytic signal of two-dimensional magnetic bodies with polygonal cross-section: Its properties and use for automated anomaly interpretation. *Geophysics*, 37(3): 507-517.
- Queiroga, C. N., Suita, M. T. F., Soares, A. C. P., Martins, M. S., Pinheiro, M. A. P.**, 2012, Síntese sobre ofiolitos: evolução dos conceitos, *R. Esc. Minas, Ouro Preto*, 65 (1), 47 - 58.
- Roest, W. R., Verhoef, J., Pilkington, M.**, 1992, Magnetic interpretation using the 3-D analytic signal: *Geophysics*, 57, 116-125
- Salem, A., Ravat, D.**, 2003, A combined analytic signal and Euler method (AN - EUL) for automatic interpretation of magnetic data, *Geophysics*, vol. 68, 1952 - 1961 p.
- Strieder, A. J., Nilson, A. A.**, 1992a, Melange ofiolítica nos metassedimentos Araxá de Abadiânia (GO) e implicações tectônicas regionais, *Revista Brasileira de Geociências*, 22(2) 204 - 215p.
- Strieder, A. J., Nilson, A. A.**, 1992b, Estudo petrológico de alguns fragmentos tect.ônicos da melange ofiolítica em Abadiânia (GO): I - O protolito dos corpos de serpentinito, *Revista Brasileira de Geociências*, 22(3) 338 - 352p.
- Valente, C. R.**, 1986. Projeto Mapas Metalogenéticos e de Previsão de Recursos Minerais: Goiânia, Folha SE.22-X-B. Brasília, CPRM, 14 p. Convênio DNPM/CPRM.
- Verduzco, B., Fairhead, J. D., Green, C. M., Mackenzie, C.**, 2004, New insights into magnetic derivatives for structural mapping: *The Leading Edge*, 23, 116-119.
- Wildfort, J.R., Bierwirth, P. N, Craig, M. A.**, 1997, Application of airborne gamma - ray spectrometry in soil/regolith mapping and applied geomorphology, *Journal of Australian Geology & Geophysics*, 17(2), 201 - 216.